Published OnlineFirst December 21, 2016; DOI: 10.1158/1078-0432.CCR-16-1971

Biology of Human Tumors

Clinical Cancer Research

Co-occurring Mutations of Tumor Suppressor Genes, *LATS2* and *NF2*, in Malignant Pleural Mesothelioma

Robin Tranchant[1,2,3,4], Lisa Quetel[1,2,3,4], Anne Tallet[1], Clement Meiller[1,2,3,4], Annie Renier[1,2,3,4], Leanne de Koning[5], Aurelien de Reynies[6], Francoise Le Pimpec-Barthes[1,2,3,4,7,8], Jessica Zucman-Rossi[1,2,3,4,8], Marie-Claude Jaurand[1,2,3,4], and Didier Jean[1,2,3,4]

Abstract

Purpose: To better define malignant pleural mesothelioma (MPM) heterogeneity and identify molecular subtypes of MPM, we focus on the tumor suppressor gene *LATS2*, a member of the Hippo signaling pathway, which plays a key role in mesothelial carcinogenesis.

Experimental Design: Sixty-one MPM primary cultures established in our laboratory were screened for mutations in *LATS2*. Gene inactivation was modeled using siRNAs. Gene and protein expressions were analyzed by quantitative RT-PCR, Western blot analysis, and reverse phase protein array. Cell proliferation, viability, apoptosis, mobility, and invasion were determined after siRNA knockdown or YAP (verteporfin), mTOR (rapamycin), and mTOR/PI3K/AKT (PF-04691502) inhibitor treatment.

Results: The *LATS2* gene was altered in 11% of MPM by point mutations and large exon deletions. Genetic data coupled with transcriptomic data allowed the identification of a new MPM molecular subgroup, $C2^{LN}$, characterized by a co-occurring mutation in the *LATS2* and *NF2* genes in the same MPM. MPM patients of this subgroup presented a poor prognosis. Coinactivation of *LATS2* and *NF2* leads to loss of cell contact inhibition between MPM cells. Hippo signaling pathway activity, mTOR expression, and phosphorylation were altered in the $C2^{LN}$ MPM subgroup. MPMs of this new subgroup show higher sensitivity to PF-04691502 inhibitor. The *MOK* gene was identified as a potential biomarker of the $C2^{LN}$ MPM subgroup and PF-04691502 sensitivity.

Conclusions: We identified a new MPM molecular subgroup that shares common genetic and transcriptomic characteristics. Our results made it possible to highlight a greater sensitivity to an anticancer compound for this MPM subgroup and to identify a specific potential biomarker. *Clin Cancer Res; 23(12); 3191–202. ©2016 AACR.*

Introduction

Malignant pleural mesothelioma (MPM) is an aggressive tumor that is resistant to conventional anticancer therapies (surgery, radiotherapy, and chemotherapy), resulting in poor prognosis and very short patient survival (an average of 12 months). Its major risk factor is past exposure to asbestos fibers, a carcinogen that induces genomic and genetic alterations (1). To improve the prognosis of this disease, there is a strong need to develop efficient therapeutic strategies, taking the molecular alterations and clinicobiological heterogeneity of tumors into account.

MPM is characterized by numerous chromosomal abnormalities, gene mutations (mainly deletions), epigenetic alterations, and specific gene expression (2). Heterogeneity of tumors was found at these different molecular levels. Concerning the genetic alteration, sequencing analyses showed that alterations mostly concern tumor suppressor genes. Mutations in *CDKN2A* (Cyclin-dependent kinase inhibitor 2A), *CDKN2B* (Cyclin-dependent kinase inhibitor 2B), *BAP1* (BRCA1 associated protein-1), and *NF2* (Neurofibromin 2) have been reported in a high percentage of MPMs. Mutations in *TP53* (Tumor protein p53) were also found but at a lower percentage (3). Recent next-generation sequencing studies did not find any frequent recurrent alterations in other tumor suppressor genes or oncogenes (4–6). A recurrent oncogenic mutation in the *TERT* promoter was previously found in our laboratory. It was the first hotspot oncogenic mutation identified in MPM (7).

We previously defined a robust MPM molecular classification consisting of two groups (C1 and C2) with different molecular profiles, gene alterations, histology subtypes, and survival outcomes. Epithelioid MPMs were found in both groups with a worse survival prognosis in the C2 group. The C1 group exhibited more

[1]Génomique Fonctionnelle des Tumeurs Solides, INSERM, UMR-1162, Equipe labellisée Ligue Contre le Cancer, Paris, France. [2]Université Paris Descartes, Sorbonne Paris Cité, Labex Immuno-oncology, Paris, France. [3]Institut Universitaire d'Hématologie, Université Paris Diderot, Sorbonne Paris Cité, Paris, France. [4]Université Paris 13, Sorbonne Paris Cité, Saint-Denis, France. [5]Translational Research Department, Institut Curie, PSL Research University, Paris, France. [6]Programme Cartes d'Identité des Tumeurs (CIT), Ligue Nationale Contre Le Cancer, Paris, France. [7]Département de Chirurgie Thoracique, Hopital Européen Georges Pompidou, Paris, France. [8]Assistance Publique-Hopitaux de Paris, Hopital Européen Georges Pompidou, Paris, France.

Note: Supplementary data for this article are available at Clinical Cancer Research Online (http://clincancerres.aacrjournals.org/).

Current address for A. Tallet: Platform of Somatic Tumor Molecular Genetics, University Hospital, F-37000, Tours, France.

Corresponding Author: Didier Jean, INSERM UMR-1162, 27, rue Juliette Dodu, Paris F-75010, France. Phone: 3301-7263-9350; Fax: 331-5372-5192; E-mail: didier.jean@inserm.fr

doi: 10.1158/1078-0432.CCR-16-1971

Published OnlineFirst December 21, 2016; DOI: 10.1158/1078-0432.CCR-16-1971

Translational Relevance

Malignant pleural mesothelioma (MPM) is a devastating therapy-resistant cancer. Knowledge of the molecular alterations and clinicobiological heterogeneity involved is critical to improve MPM therapeutic efficiency. We recently established a robust molecular MPM classification consisting of two groups characterized by different molecular profiles and survival outcomes. In the current study, we defined a new homogeneous tumor subgroup that shares common genetic alterations and similar gene expression profiles. Characterization of specific deregulated signal pathways led us to identify an anticancer compound, an inhibitor of the mTOR/PI3K/AKT pathway already used in clinical trials for other types of cancer, to target this MPM subgroup. To better select patients eligible for this targeted therapy, we also proposed a potential biomarker. Our findings highlight the importance for translational research of taking genetic alteration, transcriptomic classification, and signal pathway activation into account to establish a new therapeutic approach and to improve MPM management.

frequent *BAP1* alterations and the C2 group presented a mesenchymal phenotype (8).

The Hippo signaling pathway plays a key role in the control of organ size and in carcinogenesis by regulating cell growth and apoptosis (9). The Hippo pathway regulates the transcriptional coactivator YAP (Yes-associated protein, *YAP1* gene) activity, which is involved in MPM carcinogenesis (10, 11). Under healthy conditions, at high cell density, YAP is phosphorylated and sequestrated in the cytoplasm after interaction with 14-3-3 proteins, resulting in proteasomal degradation. At low cell density, YAP is transduced to the nucleus and interacts with several transcription factors, including TEAD family members, to promote expression of target genes that promote carcinogenesis (12). In MPM, recurrent inactivating mutations are found in members of this pathway, *NF2* and *LATS2* (large tumor suppressor 2) genes, resulting in aberrant cotranscriptional activity of YAP. However, the alteration frequency of *LATS2* in MPM remains unclear (6, 13, 14).

In the current study, we first focused on *LATS2* gene alteration on our collection of MPM primary cultures to better define the frequency and the mechanism of *LATS2* inactivation in MPM. On the basis of genetic alterations and transcriptomic classification, we identified a specific MPM molecular subgroup characterized by a co-occurring mutation in *LATS2* and *NF2*. Molecular analysis makes it possible to identify specific signal pathways deregulated in this MPM subgroup. These data allowed us to identify a specific biomarker and to highlight a greater sensitivity to an anticancer compound for this MPM subgroup.

Materials and Methods

Mesothelioma cells in culture

MPM in culture (61 cases), previously characterized for genetic alterations in key genes of mesothelial carcinogenesis (*CDKN2A*, *CDKN2B*, *BAP1*, *NF2*, and *TP53*), were primary cell lines established in our laboratory (therefore they could not be authenticated) and used in several previous studies showing their relevance to MPM primary tumors (7, 8, 15, 16). Clinicopathologic, epidemiologic, and molecular data are reported in Table 1.

siRNA-targeted knockdown

RNA interference was used to knockdown *NF2*, *LATS2*, and *YAP* expression in MPM cells by using two different siRNAs for each targeted gene. Silencer Select predesigned siRNAs were purchased from Thermo Fisher Scientific/Ambion (Supplementary Table S1). Knockdown was performed by reverse transfection of siRNA into cells using Lipofectamine RNAiMAX reagent (Thermo Fisher Scientific) according to the manufacturer's instructions. Briefly, 3×10^5 cells were seeded on 6-well plates (TPP) and transiently transfected with equal amounts of siRNA (4 nmol/L siRNA for simple transfection and 8 nmol/L for cotransfection), using 2.5 μL/mL of transfection reagent. As a control, cells were transfected without siRNA and with two untargeting siRNA (Silencer Select Negative Control #1 or #2 siRNA, Thermo Fisher Scientific/Ambion).

Cell proliferation and inhibitor assays

For proliferation, MPM cells were seeded in triplicate and transfected on 96-well plates (Corning, Falcon) at different concentrations: 5×10^3 or 1×10^4 cells/well for nonconfluent conditions and 3×10^4 cells/well for confluent conditions. For inhibitor assays, MPM cells were seeded at 1×10^4 cells/well in triplicate. Cells were treated for 48 hours with gradient concentrations of a potent YAP inhibitor (verteporfin; #S1786; Selleck Chemicals), a specific mTOR inhibitor (rapamycin; #S1039; Selleck Chemicals) or a specific mTOR/PI3K/Akt inhibitor (PF-04691502; #S2743; Selleck Chemicals). Cell proliferation was quantified by MTS assay (CellTiter 96 AQueous One Solution Cell Proliferation Assay, Promega) using an absorbance reader (FLUOstar Omega, BMG Labtechnologies). Area under curve

Table 1. Clinicopathologic and molecular characteristics of MPMs

	MPM cells in culture ($n = 61$)
Gender, *n* (%)	
Male	48 (79)
Female	13 (21)
Age (years)	
Median ± SD	65 ± 10
Range	37–89
Histology, *n* (%)	
Epithelioid	43 (74)
Biphasic	8 (14)
Sarcomatoid	6 (10)
Desmoplastic	1 (2)
Asbestos exposure, *n* (%)	
Exposed	47 (80)
Non-exposed	12 (20)
Survival (months)	
Median	10
Range	0.3–118.8
Molecular group, *n* (%)	
C1	20 (33)
C2	41 (67)
Genetic alterations, *n* (%)	
CDKN2A	46 (75)
CDKN2B	41 (67)
BAP1	30 (49)
NF2	27 (44)
TP53	6 (10)

Published OnlineFirst December 21, 2016; DOI: 10.1158/1078-0432.CCR-16-1971

(AUC) was determined by GraphPad Prism 6 software for inhibitor assays. Results were obtained from at least two independent experiments. Apoptosis assays were performed by Annexin V and propidium iodide (PI) staining (see Supplementary Methods for details).

Mutation and gene expression analysis

Genetic alterations in the *LATS2* gene in MPM cells were screened by Sanger sequencing as described previously (7, 16), using specific primers (Supplementary Table S2). Gene expression was analyzed by quantitative RT-PCR. Protein expression was determined by Western blot analysis and reverse phase protein array (RPPA) technology (see Supplementary Methods for details). RPPA was performed on 39 MPMs in culture as described previously (17) and arrays revealed with the antibodies are given in Supplementary Table S3. Raw data were normalized using NormaCurve, which normalizes for fluorescent background per spot and a total protein stain (18).

Statistical analyses

Unsupervised consensus clustering analysis of the 23 MPMs of the C2 subgroup was performed using Affymetrix HG-U133-plus-2.0 microarray data (ArrayExpress accession number E-MTAB-1719) as reported previously (8). Differentially expressed genes were identified from microarray data using the Bioconductor Limma package in the statistical program R (19). GraphPad Prism version 6 software was used to perform the other statistical tests: Mann–Whitney test for the whole MPM series data, *t* test for the siRNA experiment and log-rank test of the Kaplan–Meier plot for survival comparison. *P* values are shown in the figure as *, $P < 0.05$; **, $P < 0.01$ and ***, $P < 0.001$.

Results

Genetic alterations in the *LATS2* gene

Genetic alterations in the *LATS2* gene were studied by DNA sequence analysis using our series of 61 MPMs in culture (Table 1). *LATS2* mutations were detected in seven of the 61 MPMs in culture (11%) and consisted of three large deletions and four different point mutations (Fig. 1A; Supplementary Table S4). MPM_18 and MPM_40 showed a deletion of exon 2, and MPM_29 showed a deletion of exons 3 and 4. Two nonsense mutations were found in exon 4 of MPM_08 (c.1237C>T, p.Q413*) and MPM_14 (c.685C>T, p.Q229*). A frameshift mutation introduced a stop codon in exon 5 (c.1425delC, p.P475fs) into MPM_47. One missense mutation c.2873G>A (p.R958H) was found in exon 8 (coding for the catalytic kinase domain of the LATS2 protein) of MPM_04 with functional consequences on the protein activity, according to prediction programs. None of these mutations was previously identified in the COSMIC database (http://cancer.sanger.ac.uk/cosmic/; last access: November 16, 2016). MPM without mutation expressed *LATS2* mRNA and LATS2 protein (Fig. 1B and C). Complete loss of mRNA expression was only observed in MPM with large exon deletions (Fig. 1B). Among the seven *LATS2* mutants, only the MPM in culture with missense mutation (MPM_04) showed LATS2 protein expression (Fig. 1C).

Molecular characteristics of *LATS2* MPM mutants are shown in Fig. 1D. Mutants were mainly found in the C2 molecular tumor group (6/7 cases). No significant association was found between *LATS2* mutations and genetic alterations in other genes involved in mesothelial carcinogenesis (*CDKN2A*, *CDKN2B*, *BAP1*, *NF2*, and *TP53*). Interestingly, five of the seven *LATS2* mutants (8% of all the MPM) are also mutated for *NF2*, another member of the Hippo signaling pathway, which is otherwise altered in 27 MPMs in culture (44%). We focused on these MPM with *LATS2*/*NF2* co-occurring mutations, all found in the C2 molecular group.

Molecular subgroup of MPM with *LATS2*/*NF2* co-occurring mutations

Three MPMs with *LATS2*/*NF2* co-occurring mutations (MPM_04, MPM_08, and MPM_29) were part of a previous transcriptomic analysis (8). In the current study, we performed an unsupervised consensus classification of the C2 group (Fig. 2A). The three MPMs with co-occurring mutations were found in a C2 subgroup and shared similar transcriptomic profiles with two other MPMs (MPM_18 and MPM_38). MPM_18 is only mutated in *LATS2* gene and MPM_38 is wild-type for both *LATS2* and *NF2*. As it is known *WWTR1* [encoding the TAZ transcription coactivator closely related to YAP (12)] may play a role in the function of the Hippo pathway, gene expression of both *YAP1* and *WWTR1* was analyzed in the MPM series. MPM in culture have a relatively homogeneous expression for both genes except MPM_38, which is characterized by a strong overexpression of *WWTR1* gene (Supplementary Fig. S1). This subgroup of five MPMs is further referred to as $C2^{LN}$. The two MPMs with *LATS2*/*NF2* co-occurring mutations (MPM_47 and MPM_40) that were not included in the transcriptomic analysis, but classified in the C2 group using gene predictors (8), were integrated into the $C2^{LN}$ MPM subgroup for the subsequent analyses.

Among the MPM in the $C2^{LN}$ subgroup, three were sarcomatoid, two epithelioid, and one biphasic. No significant difference was found between the $C2^{LN}$ MPM subgroup and other MPM patients concerning gender, age, or asbestos exposure. Overall survival of the $C2^{LN}$ subgroup of MPM patients was lower compared with overall *NF2*-mutated MPM and other MPM patients ($P = 0.02$; Fig. 2B).

Effect of *LATS2*/*NF2* coinactivation on proliferation, invasion, and migration of MPM cells

Simple or double inactivation of *LATS2* and *NF2* was simulated in three different MPM wild-type cells for *LATS2* and *NF2* genes (MPM_07, MPM_32 and MPM_34) using efficient siRNA (Supplementary Fig. S2). Cell proliferation was measured in si*LATS2*- and/or si*NF2*-transfected cells and compared with siControl-transfected cells. A significant increase of proliferation in MPM_34 cells transfected with si*LATS2*/*NF2* was observed only when the cells reached the confluent state (Fig. 2C). Consistently, in the three MPM cells transfected with si*LATS2*/*NF2*, no effect was observed up to a confluent state (Supplementary Fig. S3A) but a proliferation increase of 30% to 50% was found at confluence (Fig. 2D). In agreement with these observations, foci formation was observed when MPM of the $C2^{LN}$ subgroup were maintained at confluence (Supplementary Fig. S3B). After single inactivation of *LATS2* or *NF2*, a slight increase was observed in only two MPM in culture (around 20% for MPM_07 and MPM_32) with *LATS2* siRNA, and no effect on proliferation was observed with *NF2* siRNA (Fig. 2D). Inactivation by siRNA of both *LATS2* and *NF2* did not modify cell migration or invasion (Supplementary Fig. S3C and S3D).

Published OnlineFirst December 21, 2016; DOI: 10.1158/1078-0432.CCR-16-1971

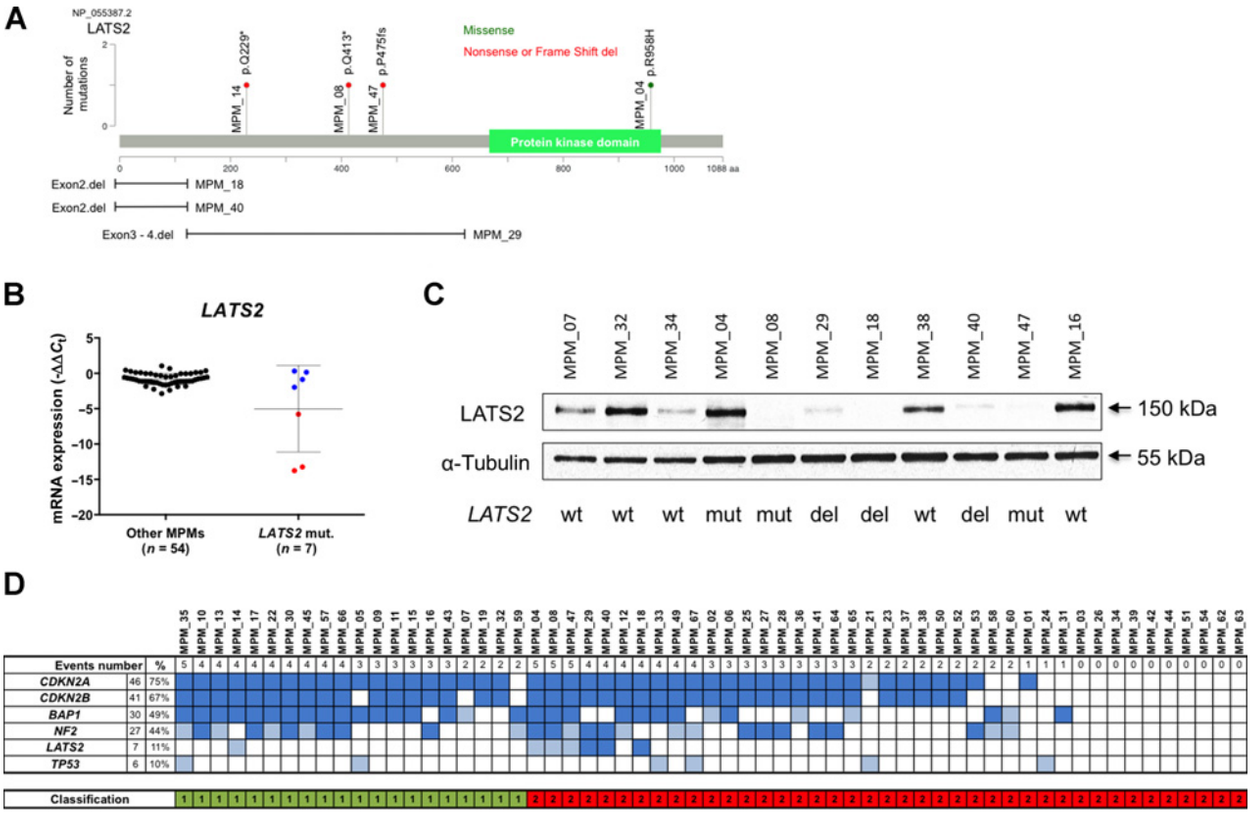

Figure 1.

LATS2 alterations in MPM cells in culture. **A,** Schematic representation of the *LATS2* gene with genetic alterations characterized by Sanger sequencing. Large exon deletions are shown at the bottom. **B,** *LATS2* mRNA expression was measured by qRT-PCR. Dot plots of $-\Delta\Delta C_t$ values are shown for wild type (black), mutated (blue), and exon-deleted MPM (red). **C,** Cell extracts from wild-type and *LATS2* MPM mutants were analyzed by Western blot analysis using anti-LATS2 antibody. α-Tubulin expression was used as a control. wt, wild type; mut, mutated; del, deletion. **D,** Heatmap representation of genetic alteration profile of MPM in culture ($n = 61$) for *CDKN2A, CDKN2B, BAP1, NF2, LATS2*, and *TP53* genes. Dark blue is for exon deletions and light blue for point mutations. The MPM molecular classification is shown at the bottom: C1 group (green) and C2 group (red).

Pathway deregulation of the C2^{LN} subgroup MPM

To explore signaling pathways impaired by *LATS2*/*NF2* co-occurring mutations, we compared phosphorylation levels of 40 proteins, key members of several major signaling pathways, between the C2^{LN} MPM subgroup and the other MPMs by RPPA (Supplementary Table S3). The phosphorylation level was significantly decreased in the C2^{LN} MPM subgroup for YAP, the serine/threonine protein kinase mTOR, and the EPHA2 receptor tyrosine factor in the C2^{LN} MPM subgroup (Fig. 3A; Supplementary Fig. S4A and S4B).

To validate the decrease of YAP phosphorylation in MPM of the C2^{LN} subgroup, we studied YAP phosphorylation status by Western blot analysis. A slightly lower ratio of total Phospho-YAP/YAP was found in the C2^{LN} MPM subgroup compared to the *NF2*-mutated MPM and other MPMs (Fig. 3B; Supplementary Fig. S4C). All the MPM of the C2^{LN} subgroup show a relative high percentage of nuclear YAP relative to total cell YAP in comparison with the other MPMs (Supplementary Fig. S5A). The mRNA expressions of three YAP potential targeted genes [*CTGF* (connective tissue growth factor), *ANKRD1* (ankyrin repeat domain 1) and *CYR61* (cysteine-rich, angiogenic inducer, 61)] were also studied. We first verified that these three genes are YAP-targeted genes in MPM by demonstrating that *CTGF, ANKRD1*, and *CYR61* expressions were significantly decreased after *YAP1* knockdown by siRNA either in three MPMs of the C2^{LN} subgroup (MPM_08, MPM_40, and MPM_47) or in another MPM (MPM_32; Supplementary Fig. S5B and S5C). *CTGF, ANKRD1*, and *CYR61* expressions were then compared in 61 MPMs in culture, including MPM of the C2^{LN} subgroup, *NF2*-mutated MPM, and other MPMs. A slightly increased expression of these three genes was found in the C2^{LN} MPM subgroup in subconfluent cells (Fig. 3C) and was enhanced when the cells were confluent (Supplementary Fig. S5D). Verteporfin, a potent YAP inhibitor, strongly inhibited cell viability in all MPMs (Supplementary Fig. S5E). The MPM of the C2^{LN} subgroup were more resistant to Verteporfin than other MPMs (Supplementary Fig. S5F). Overall, these data suggest a high cotranscriptional activity of *YAP* and a low Hippo pathway activity in MPM of the C2^{LN} subgroup.

mTOR phosphorylation and total protein expression were also analyzed by Western blot analysis (Fig. 3D and E; Supplementary Fig. S4C). RPPA data on mTOR phosphorylation were confirmed, suggesting that mTOR is less active in the C2^{LN} MPM subgroup (Fig. 3D). A decrease in mTOR expression was also observed in the C2^{LN} subgroup, indicating that lower phosphorylation of mTOR is linked to a lower protein expression (Fig. 3E).

Published OnlineFirst December 21, 2016; DOI: 10.1158/1078-0432.CCR-16-1971

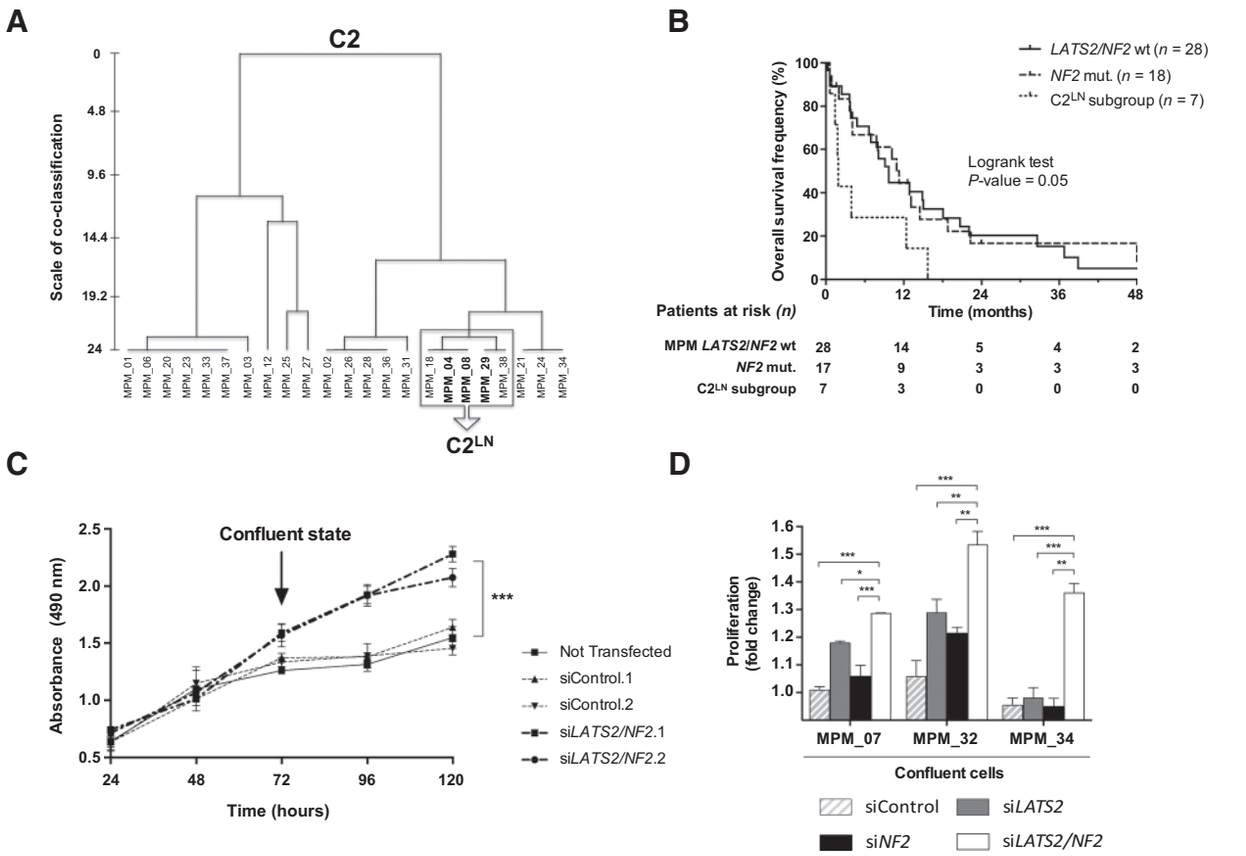

Figure 2.

Characteristics of the $C2^{LN}$ MPM subgroup and effect of *LATS2/NF2* inactivation on MPM proliferation. **A,** Hierarchical unsupervised consensus classification of 23 MPMs in culture from the C2 group was performed on gene expression profiles. The consensus dendrogram is shown. The three *LATS2/NF2* comutants (bold black line) are included in a specific subgroup referred to as $C2^{LN}$. **B,** Differences between overall survival of the *LATS2/NF2* wild-type MPMs, *NF2* MPM mutants, and the $C2^{LN}$ MPM subgroup are shown. The Log-rank test *P* value is indicated. **C,** One *LATS2/NF2* wild-type MPM (MPM_34) was transfected with siControl or both si*LATS2* and si*NF2*. Proliferation was followed by MTS assay for 120 hours. Results are expressed as the mean ± SEM of one representative experiment. **D,** Three *LATS2/NF2* wild-type MPMs were transfected with siControl, si*LATS2*, si*NF2*, or both si*LATS2* and si*NF2*. Two different siRNAs for each targeted gene were used. Proliferation was quantified by MTS assay 96 hours after siRNA transfection. The mean of the two different siRNAs for each targeted gene was calculated and compared with an untransfected control. The histogram shows fold changes ± SD of one representative experiment. Statistical comparisons were performed on two or more independent experiments compared with siControl.

Targeted treatment of the $C2^{LN}$ subgroup MPM

The low expression and phosphorylation of the mTOR protein allowed us to target mTOR in the $C2^{LN}$ MPM subgroup to determine whether mTOR inhibitors could affect cell viability. We selected a specific mTOR inhibitor (rapamycin) and an mTOR/PI3K/AKT inhibitor (PF-04691502). Treatment with rapamycin caused a slight decrease of cell viability in most of the cell lines, even at high concentrations (5%–48% at 10 μmol/L; Supplementary Fig. S6A and S6B). In contrast, PF-04691502 significantly inhibited cell viability in all MPM (47%–92% at 10 μmol/L), but PF-04691502 sensitivity was variable between MPM in culture (Fig. 4A). Interestingly, the MPMs of the $C2^{LN}$ subgroup were more sensitive to PF-04691502 than other MPMs (Fig. 4A and B). Using two MPMs of the $C2^{LN}$ subgroup, we confirmed that PF-04691502 inhibits mTOR by analyzing phosphorylation of mTOR downstream targets, 4E-BP1, p70 S6 kinase (P70-S6K), and S6 ribosomal protein (S6R; Supplementary Fig. S6C). We used Annexin V/propidium iodide staining assay to determine the PF-04691502 mechanism of cell death in two representative MPMs. After treatment with gradient concentrations of PF-04691502, the apoptotic cells were increased from 13.2% to 85.4% in MPM of the $C2^{LN}$ subgroup (MPM_29) and from 12.9% to 24% in other MPM (MPM_17; Fig. 4C and D).

Identification of *MOK*, a specific biomarker of the $C2^{LN}$ MPM subgroup

To define a specific biomarker of the $C2^{LN}$ MPM subgroup, we compared mRNA expression between the $C2^{LN}$ MPM subgroup and the other MPMs using previously reported transcriptomic data (ref. 8; Fig. 5A). A list of 42 deregulated genes was obtained with an adjusted $P < 0.01$ (Supplementary Table S5). We selected four upregulated genes (*MOK*, *CHRDL1*, *TXNRD2*, and *PTPRB*) and one downregulated gene (*NEO1*), based on fold change and gene function. The mRNA expression level of these genes was further analyzed by qRT-PCR in all 61 MPM in culture. *MOK*, *CHRDL1*, *PTPRB*, and *NEO1* showed highly significant deregulation in the $C2^{LN}$ MPM subgroup (Fig. 5B;

Published OnlineFirst December 21, 2016; DOI: 10.1158/1078-0432.CCR-16-1971

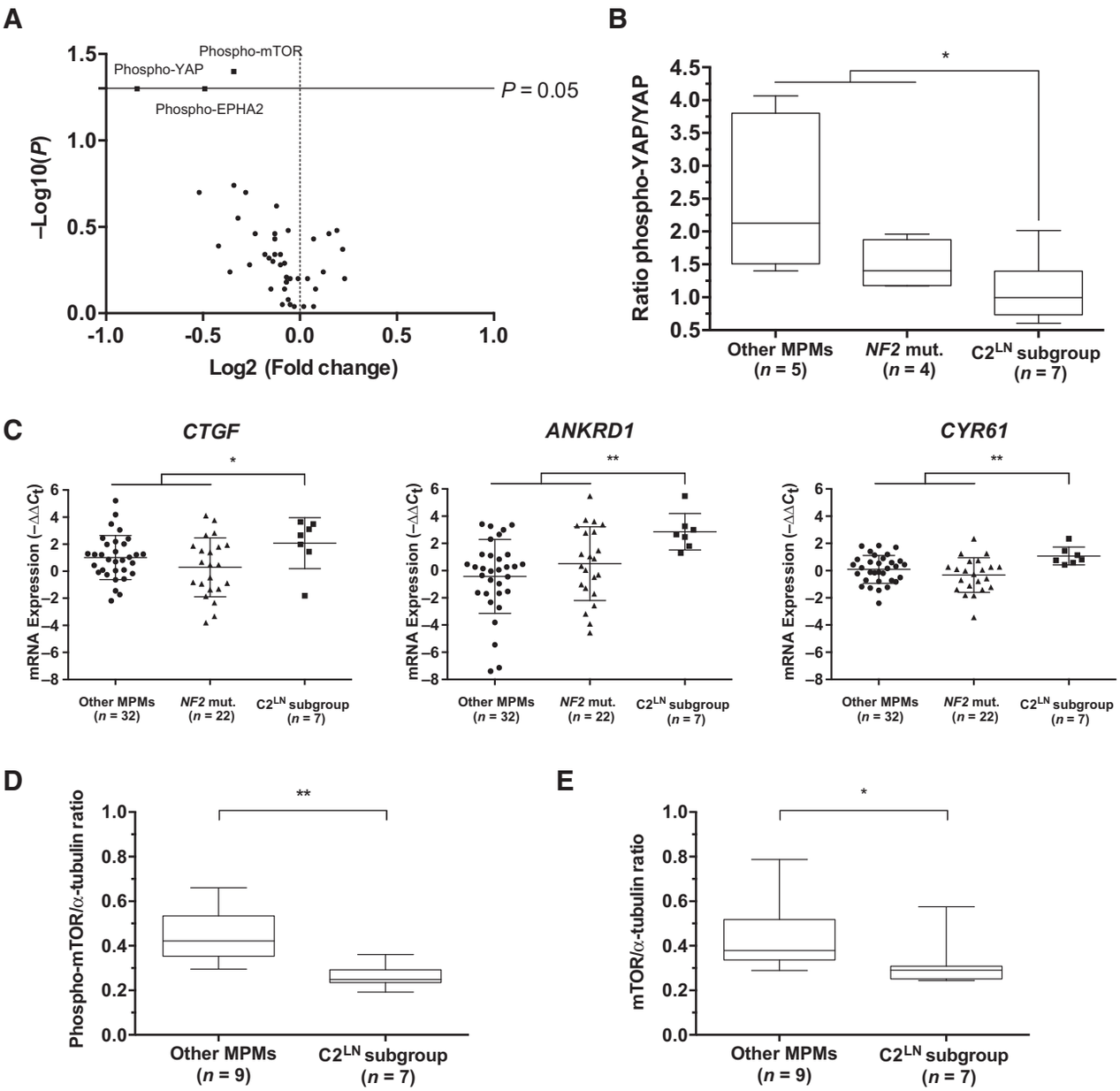

Figure 3.

Signaling pathway activation in the C2^{LN} MPM subgroup. **A,** RPPA analysis was performed on cell extracts of 39 MPMs using antibodies specific to 40 phosphorylated proteins, key members of several major signaling pathways. The volcano plot of RPPA data comparing the C2^{LN} MPM subgroup to other MPMs is shown. **B** and **D–E,** Cell extracts from the C2^{LN} MPM subgroup, *NF2* MPM mutants and other MPMs were analyzed by Western blot analysis. The boxplot shows the Phospho-YAP/YAP ratio (**B**) and Phospho-mTOR and mTOR ratios normalized to α-tubulin (**D–E**) determined from Western blot signal intensity. **C,** mRNA expressions of Hippo pathway target genes (*CTGF*, *ANKRD1*, and *CYR61*) were measured by qRT-PCR. Dot plots of $-\Delta\Delta C_t$ values are shown for the C2^{LN} MPM subgroup, *NF2* MPM mutants, and other MPMs. Statistical comparisons were performed by comparing the C2^{LN} MPM subgroup to *NF2* MPM mutants and other MPMs.

Supplementary Fig. S7A). In si*LATS2* and/or si*NF2*-transfected MPMs, only *MOK* (MAP overlapping kinase) mRNA was specifically upregulated after knocking down both *LATS2* and *NF2*, indicating that the *MOK* gene is a potential biomarker of the C2^{LN} MPM subgroup (Fig. 5C; Supplementary Fig. S7B). Furthermore, *MOK* mRNA expression was not modified by *YAP1* inhibition using specific siRNA in three MPMs of the C2^{LN} subgroup, suggesting that *MOK* expression was regulated by *LATS2*/*NF2* inactivation independently of YAP activity (Supplementary Fig. S7C). Moreover, we found a significant correlation between *MOK* mRNA expression and normalized AUC of PF-04691502–treated MPM cells, suggesting that *MOK* expression could also be a predictor of PF-04691502 sensitivity in MPMs (Fig. 5D).

Published OnlineFirst December 21, 2016; DOI: 10.1158/1078-0432.CCR-16-1971

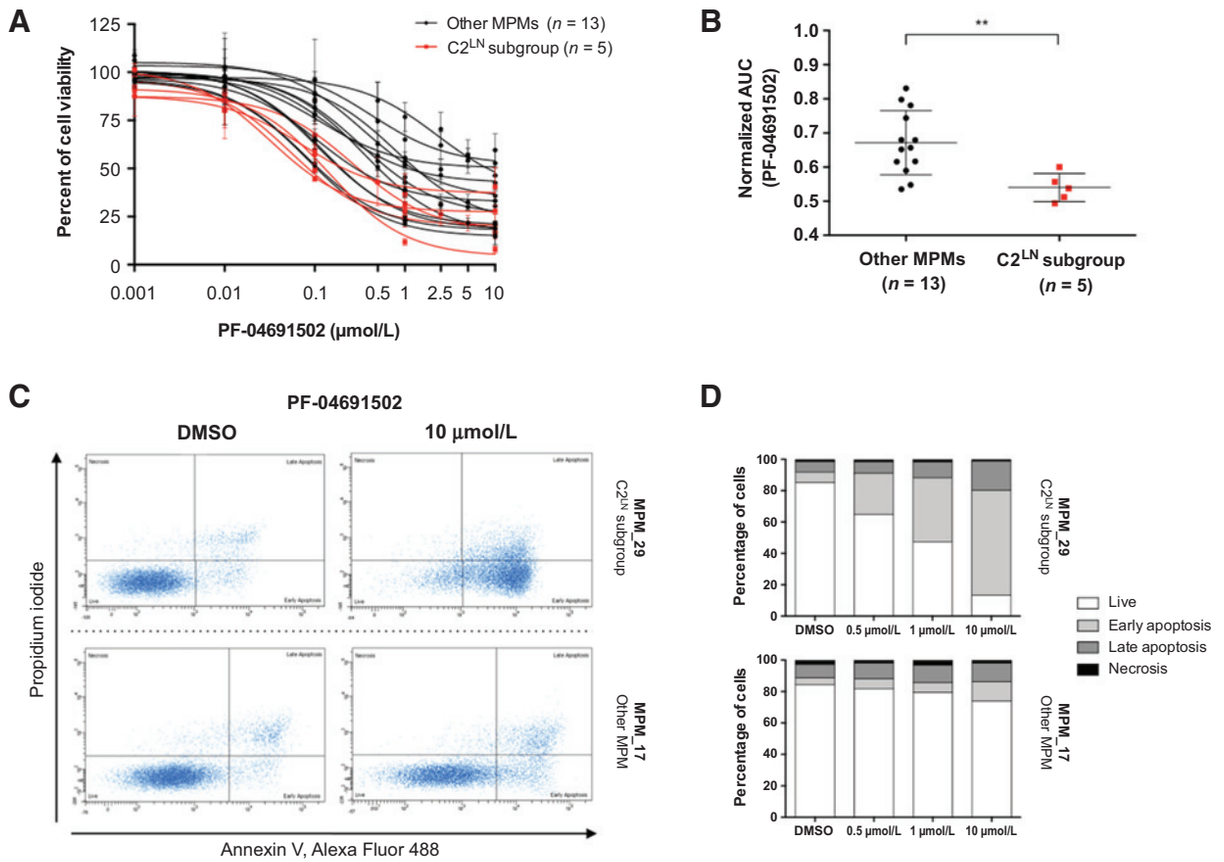

Figure 4.

Effect of mTOR/PI3K/AKT inhibitor on cell viability. **A,** Cell viability curves of 18 MPMs were determined in the presence of a gradient concentration of PF-04691502, a mTOR/PI3K/AKT inhibitor. Each point represents the mean ± SD of two independent experiments. **B,** PF-04691502-normalized AUCs of each MPM are compared between the $C2^{LN}$ MPM subgroup and other MPMs. **C** and **D,** One MPM of the $C2^{LN}$ subgroup (MPM_29) and another MPM (MPM_17) were treated with gradient concentration of PF-04691502 for 48 hours. MPM cells were stained with Annexin V-Alexa Fluor 488 and propidium iodide. Early apoptosis, late apoptosis, and necrosis were determined using flow cytometry (**C**). The percentage of cells in the lower left quadrant (live cells), the lower right quadrant (early apoptotic cells), the upper right quadrant (late apoptotic cells), and the upper left quadrant (necrotic cells) was quantified at a gradient concentration of PF-04691502 (**D**). Results are shown for one representative experiment.

Discussion

Genetic alterations in members of the Hippo pathway are frequent in MPM cells. The most frequently mutated gene is *NF2*, an upstream regulator, with rates of 40% to 60% (20). Mutations in *LATS2* were first described by Murakami and colleagues (13) at a high rate of mutation (35%, 7/20 MPM in culture), which was not confirmed in two larger series of MPM tumor samples (4%, 2/53 MPM tumor samples; 3%, 6/202 tumor samples; refs. 6, 14). In the Murakami series, 4 of 7 genetic alterations were large biallelic deletions (20%, 4/20 MPM in culture) and 3 of 7 were point mutations (15%, 3/20 MPM in culture). In the current larger series of 61 MPM cells in culture, a mutation rate of 11% of overall mutations (6% of point mutations and 5% of large deletions) was found. Large deletions represent 42% of overall mutations for *LATS2* in our series. Most sequencing methods do not make it possible to identify large biallelic deletions in tumor samples due to the presence of normal cells, in contrast to cell lines. Our sequencing data confirm that the point mutation rate of *LATS2* is around 5% in MPM and underlines the need to evaluate large biallelic deletions by FISH or other analyses to have a correct evaluation of *LATS2* genetic alterations in MPM tumor samples. Analysis of *LATS2* mRNA and protein expression in our MPM series suggests that genetic alterations are the main mechanism of inactivation for this gene. Genetic alterations of other Hippo pathway members have been described for *LATS1* (large tumor suppressor 1), *SAV1* (salvador homolog 1), *MST1*, *MST2* (macrophage stimulating 1 and 2), *RASSF1* (ras association domain family member 1) and *STK3* (serine/threonine kinase 3), but their mutation frequencies were very low (4, 6, 13, 14, 21). As *LATS1* gene is a homologue of *LATS2*, we analyzed *LATS1* mRNA and protein expression by RT-qPCR and Western blot analysis, respectively, in our MPM series (data not shown). We observed similar mRNA expression of *LATS1*, but variable protein expression. Absence of LATS1 protein expression was observed in three of seven *LATS2*-mutated MPMs and one of 34 wild-type MPMs, showing a significant association ($P = 0.01$)

Published OnlineFirst December 21, 2016; DOI: 10.1158/1078-0432.CCR-16-1971

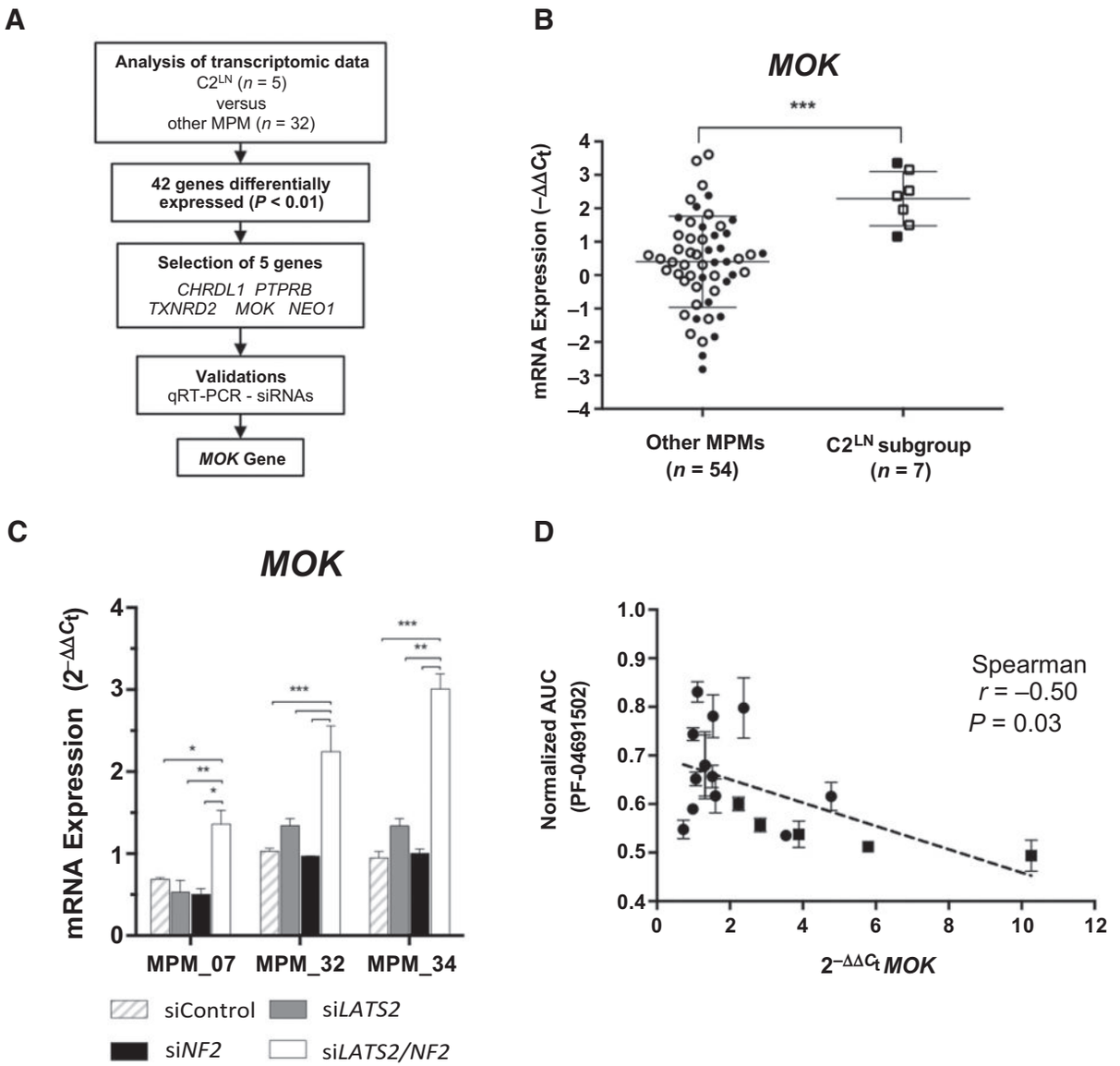

Figure 5.

Identification of a $C2^{LN}$ MPM subgroup biomarker. **A,** Diagram of selection, from transcriptomic data, of deregulated genes between the $C2^{LN}$ MPM subgroup and other MPMs. **B** and **C,** *MOK* mRNA expressions were measured by qRT-PCR. Dot plots of $-\Delta\Delta C_t$ values are shown for the $C2^{LN}$ MPM subgroup and the other MPMs. Open circles and open squares represent MPM included in transcriptomic analysis; closed circles and closed squares represent MPM not included in transcriptomic analysis (**B**). Three *LATS2/NF2* wild-type MPMs were transfected with siControl, si*LATS2*, si*NF2*, or both si*LATS2* and si*NF2*. Two different siRNAs for each targeted gene were used. The mean of $2^{-\Delta\Delta C_t}$ obtained from the two different siRNAs of each targeted gene was calculated. The histogram shows the mean ± SD of one representative experiment. Statistical comparisons were performed on two or more independent experiments compared with siControl (**C**). **D,** Correlation between *MOK* mRNA expression and PF-04691502-normalized AUCs of 18 MPMs in culture. Each point represents the mean ± SD of two independent experiments. Circle, other MPMs; square, $C2^{LN}$ MPM subgroup.

between *LATS2* gene mutation and LATS1 expression loss by a post-transcriptional mechanism. This observation needs to be confirmed in a larger series.

We identified co-occurring mutations of the two Hippo pathway members, *LATS2* and *NF2*, in 8% of MPM samples. It is generally expected that a single tumor has alterations in only one member of a given signal pathway. However, the discovery of an increasing number of mutated genes in human cancers has led to the identification of genes with co-occurring mutations, which mapped to the same pathway (22). *LATS2/NF2* co-occurring mutants were also found in the Murakami series of MPM in culture (15%), and in the Miyanaga (4%), Bott (2%), and Bueno (1%) tumor samples series (6, 13, 14, 21). These co-occurring mutations were more frequently detected in MPMs in culture than

Published OnlineFirst December 21, 2016; DOI: 10.1158/1078-0432.CCR-16-1971

in MPM tumor samples, consistent with the poor detection of large biallelic deletions in MPM tumor samples. Next-generation sequencing (NGS) approaches are very efficient to detect variants, but may fail to identify large deletions because of the presence of contaminating normal stromal and immune cells in the tumor sample. Large deletions are common in MPM: *NF2* is also frequently altered by large exon biallelic deletion (59% in our series). An integrated approach is required to correctly estimate the frequency of *LATS2/NF2* co-occurring inactivation in tumor samples including multiplex ligation-dependent probe amplification (MLPA), FISH, and IHC. Data mining of DNA-sequencing studies shows other co-occurring alterations in other Hippo pathway members, even they are infrequent in MPM (*LATS2/MST1*, *LATS2/RASSF1*, *LATS2/SAV1*, *NF2/LATS1*, *NF2/RASSF1*, *NF2/SAV1*; refs. 6, 13, 14, 21). Furthermore, analysis of large-scale cancer genomics datasets of the cBioPortal database (http://www.cbioportal.org/, last access: November 16, 2016) did not identify other associations between *LATS2* and *NF2* gene mutations in other cancer types due to their low mutation frequencies. Consequently, *LATS2* and *NF2* co-occurring mutants seem to be relevant and specific to MPM carcinogenesis.

In addition, we found that *LATS2/NF2* MPM mutants clustered in a specific $C2^{LN}$ subgroup of the C2 group, using the same clustering approach that led to the identification of the C1/C2 groups (8). Consequently, these mutants share a similar transcriptomic profile, suggesting a common mechanism of carcinogenesis. It is noteworthy that it is the first MPM subgroup for which such a strong link between a mutation profile and gene expression signature is highlighted. We previously described a significant association between *BAP1* gene mutation and the C1 group (8), but unsupervised consensus classification of the C1 group did not distinguish *BAP1*-mutated MPM from *BAP1* wild-type MPM (data not shown). Furthermore, a recent clustering analysis based on transcriptomic data of large MPM tumor series did not reveal a strong association between gene mutations and transcriptomic clusters (6).

Two other MPMs in culture (MPM_18 and MPM_38) are also present in the $C2^{LN}$ MPM subgroup. In MPM_18, the *LATS2* gene is altered by exon deletion, but no genetic alteration in *NF2* gene was identified and *NF2* expression was detected both at the mRNA and protein level (data not shown). Regulation of *NF2* in MPM may occur at different levels, including the post-translational mechanism. It was shown that *NF2* is rendered inactive by phosphorylation of Ser518 (23). This might be the case in MPM_18. MPM_38 has no mutation in *NF2* and *LATS2* genes, but show a strong overexpression of *WWTR1* that could support its presence in the $C2^{LN}$ MPM subgroup.

Our data suggest that coinactivation of *LAST2* and *NF2* modulates MPM proliferation. *NF2* is a key gene of mesothelial carcinogenesis. Inactivation of *Nf2* in mice favored mesothelioma formation after exposure to asbestos, showing that it is driver gene of asbestos-induced mesothelial carcinogenesis (24). However, spontaneous mesothelioma is infrequent in *Nf2* homozygous conditional knockout mice, revealing that other genetic alterations are needed for MPM formation (25). It was shown that *NF2* re-expression inhibits invasiveness in two human mesothelioma cell lines (26), but inhibition by siRNA of *NF2* did not modify the invasion property of our MPMs in culture *in vitro*. It was also shown that the re-expression of *NF2* or *LATS2* separately inhibited proliferation in MPM cell lines (13, 27). However, our data show that single inactivation of either *NF2* or *LATS2* did not affect proliferation in three *NF2* wild-type MPMs in culture. On the other hand, coinactivation of *LAST2* and *NF2* led to a loss of contact inhibition, as shown by increased proliferation of siRNA knockdown cells at confluence and foci formation in *LATS2/NF2* MPM mutants. Loss of contact inhibition may promote tumor growth and is consistent with the worse prognosis of patients in the $C2^{LN}$ MPM subgroup compared with other MPM patients. Modeling of *LATS2* and *NF2* inactivation in mice would make it possible to better understand their contribution to MPM progression.

Identification of specific biomarkers of tumor subgroup, sharing similar molecular characteristic, is essential to select patients for target therapy. Gene expression–based biomarkers are especially useful for molecular subgroups relying on various or complex genetic alterations, whose identification by sequencing in tumor samples is problematic, such as the $C2^{LN}$ MPM subgroup. We identified the *MOK* gene as a specific biomarker overexpressed in the $C2^{LN}$ MPM subgroup. Unfortunately, we assayed several anti-MOK commercial antibodies, but none was able to accurately detect MOK protein expression. Nevertheless, analysis of gene expression on frozen tumors using RT-qPCR or on formalin-fixed paraffin-embedded tumors using multiplexed hybridization assay (NanoString nCounter system) should contribute to better identify patients with MPM tumors of the $C2^{LN}$ subgroup. Interestingly, *MOK* overexpression was also associated with poor prognosis in hepatocellular carcinoma patients (28). *MOK* overexpression is induced by the simultaneous siRNA knockdown of *LATS2* and *NF2* and not of *YAP1*, demonstrating that coinactivation of *LATS2* and *NF2* leads to gene deregulation independently of YAP. *MOK* is a member of the MAP kinase family and considered as a tumor-associated antigen (RAGE-1) in renal carcinoma cells (29) and in some MPMs (30). To date, the function of *MOK* in carcinogenesis remains largely unknown. *MOK* was found to decrease the cell invasive ability of hepatocellular carcinoma cells (28). We attempted to knockdown *MOK* expression using at least six different siRNAs from two different manufacturers. Unfortunately, *MOK* expression inhibition by siRNA was only partial and we were not able to evaluate its contribution to the proliferation and invasion of MPM cells.

In the current study, we identified specific signaling pathways deregulated in the $C2^{LN}$ MPM subgroup. As expected, we observed a decrease of Hippo signaling pathway activity (decrease of YAP phosphorylation and overexpression of *CTGF*, *CYR61* and *ANKRD1*, described previously (31, 32), and confirmed as YAP target genes by *YAP1* knockdown in MPM), not only in comparison with MPM without mutation in members of this pathway, but also in MPM with mutation solely in the *NF2* gene. Furthermore, the MPM of the $C2^{LN}$ subgroup were more resistant to Verteporfin, a potent YAP inhibitor, which disrupts YAP–TEAD interactions (33), than other MPMs, consistent with higher YAP activity in the $C2^{LN}$ subgroup. It was previously suggested that MPM cells with *NF2* inactivation alone showed relatively modest YAP activation, and additional alterations of other molecules such as *SAV1*, *KIBRA*, *LATS1/2*, and *AJUBA* lead to the enhancement of YAP activation (34). This hypothesis is supported by our data on *LATS2/NF2* MPM mutants and on *NF2* MPM mutants, which showed a heterogeneous mRNA expression of YAP target genes compared with the $C2^{LN}$ MPM subgroup

However, the Hippo pathway is not the only signaling pathway altered in the $C2^{LN}$ MPM subgroup. Our findings are consistent

Published OnlineFirst December 21, 2016; DOI: 10.1158/1078-0432.CCR-16-1971

with a deregulation of mTOR in the $C2^{LN}$ MPM subgroup. mTOR is a serine/threonine kinase that belongs to the PI3K/AKT/mTOR signaling pathway and is often activated in MPM (20). It was suggested that the loss of merlin, encoded by the *NF2* gene, causes activation of mTOR signaling by studying 4E-BP1 and p70-S6-Kinase phosphorylation but not mTOR phosphorylation and expression (35). We analyzed, by Western blot analysis, the phosphorylation of 4E-BP1, p70-S6-Kinase, and S6-Ribosomal-protein using the MPM panel of Supplementary Fig. S4C (data not shown). We did not find significant difference in the phosphorylation level of these three proteins between the nine *NF2*-mutated MPM and the seven wild-type MPMs. Our data show that mTOR phosphorylation is downregulated in the $C2^{LN}$ MPM subgroup. This downregulation is linked to a decrease of mTOR expression at the protein level, but not at the mRNA level. No difference was found in mRNA expression between the $C2^{LN}$ MPM subgroup and other MPMs in our transcriptomic data (data not shown). Little is currently known about mTOR post-translational regulation and protein degradation. mTOR is targeted for ubiquitination and proteasomal degradation by binding to the E3 ubiquitin ligase FBXW7 (F-box/WD repeat-containing protein 7; ref. 36). Lysosomal degradation is another mechanism of mTOR protein expression regulation (37). Further studies are needed to understand the decrease of mTOR expression and, consequently, activity in the $C2^{LN}$ MPM subgroup.

To identify anticancer compounds specific to the $C2^{LN}$ subgroup of MPM, we then focused on mTOR inhibitors. Rapamycin, a specific mTOR inhibitor, showed a slight effect on MPM cell viability (inhibition of 20%–30%). A previous study using this inhibitor on several MPM cell lines also revealed inhibition of cell growth up to only 30% after 48 hours of treatment, except in one cell line (35). Furthermore, recent results of a phase II clinical trial showed that inhibition of mTOR alone by everolimus (a rapamycin derivate) has a limited effect in MPM patients (38). The inefficiency of rapamycin could be explained by the activation of an AKT feedback after mTOR inactivation (39). In MPM, it was shown that rapamycin strongly inhibited mTOR activity in three MPM cell lines, but was associated with an increase of AKT activation (40). Dual inhibition of mTOR and PI3K/AKT seemed to be more efficient than single mTOR inhibition, with a significant effect on proliferation and survival of MPM cell lines, as recently described (41, 42). In agreement with these studies, PF-04691502, an mTOR/PI3K/AKT pathway inhibitor (43), strongly affected the viability of our MPMs in culture. Furthermore, MPMs of the $C2^{LN}$ subgroup were more sensitive than other MPM to PF-04691502 treatment. This result could be explained by the lower mTOR protein expression and activity in this subgroup, increasing the efficiency of this ATP-competitive dual inhibitor of mTOR and PI3K. PF-04691502 treatment affects cell viability in MPMs and apoptotic cells were detected in MPM_29 and two other sensitive cell lines (data not shown). Our data suggest that induction of apoptosis by PF-04691502 contributes to affect cell viability in sensitive MPMs in culture, as has been described in other tumor cell types (44). However, the plateau observed in cell viability at higher drug concentrations in most of the MPMs in culture also indicates contribution of growth arrest and autophagy. Interestingly, we found a correlation between *MOK* mRNA expression and PF-04691502 sensitivity, suggesting that *MOK* could be used as a biomarker of the $C2^{LN}$ MPM subgroup as well as of PF-04691502 sensitivity. PF-04691502 was already studied in phase I and phase II clinical trials for several advanced cancers and recurrent endometrial cancer (45, 46), which will facilitate the clinical transfer to MPM patients, especially to patients with *LATS2* and *NF2* mutations. Nevertheless, before considering a clinical transfer in MPMs, the therapeutic value of PF-04691502 should be evaluated in preclinical animal models in relevant heterotopic and orthotopic xenograft models.

In conclusion, we clarified *LATS2* alterations in MPMs and identified a specific MPM molecular subgroup, $C2^{LN}$, characterized by frequent co-occurring mutations in *LATS2* and *NF2*, two members of the Hippo signaling pathway. Patients of the $C2^{LN}$ subgroup had a poor survival prognosis, possibly in relation to a better propensity of tumor cells to grow independently of cell–cell contact inhibition. The Hippo signaling pathway and mTOR protein expression were altered in the $C2^{LN}$ MPM subgroup. This new subgroup is more sensitive to mTOR/PI3K/AKT pathway inhibitors. We identified the *MOK* gene as a potential biomarker of MPM patients of the $C2^{LN}$ subgroup and mTOR/PI3K/AKT pathway inhibitor sensitivity. Our data demonstrate the importance of combining molecular classification and genetic alterations to define a new molecular subgroup and a new potential therapeutic strategy.

Disclosure of Potential Conflicts of Interest

No potential conflicts of interest were disclosed.

Authors' Contributions

Conception and design: R. Tranchant, F.L. Pimpec Barthes, J. Zucman-Rossi, M.-C. Jaurand, D. Jean

Development of methodology: R. Tranchant, C. Meiller, A. Renier, F.L. Pimpec Barthes

Acquisition of data (provided animals, acquired and managed patients, provided facilities, etc.): R. Tranchant, L. Quetel, A. Tallet, A. Renier, L. de Koning

Analysis and interpretation of data (e.g., statistical analysis, biostatistics, computational analysis): R. Tranchant, A. Tallet, L. de Koning, A. de Reynies, M.-C. Jaurand, D. Jean

Writing, review, and/or revision of the manuscript: R. Tranchant, L. de Koning, M.-C. Jaurand, D. Jean

Administrative, technical, or material support (i.e., reporting or organizing data, constructing databases): C. Meiller, A. Renier

Study supervision: F.L. Pimpec Barthes, J. Zucman-Rossi, M.-C. Jaurand, D. Jean

Acknowledgments

The authors thank the members of the IUH technological platform for their help with flow cytometry (Niclas Setterblad, Christelle Doliger, and Sophie Duchez), the Institut Curie RPPA platform for acquisition of RPPA data (Aurélie Cartier, Bérengere Ouine, and Audrey Criqui), and the Institut Curie bioinformatics platform for bioinformatics support (Patrick Poullet, Stéphane Liva, and Philippe Hupé).

Grant Support

This work was supported by INSERM, the Fondation ARC pour la recherche sur le cancer, the Ligue Contre le Cancer (Ile de France and Oise committees), the Groupement des Entreprises Françaises dans la Lutte contre le Cancer (GEFLUC), and the Chancellerie des Universités de Paris (Legs POIX).

The costs of publication of this article were defrayed in part by the payment of page charges. This article must therefore be hereby marked *advertisement* in accordance with 18 U.S.C. Section 1734 solely to indicate this fact.

Received August 5, 2016; revised November 18, 2016; accepted December 9, 2016; published OnlineFirst December 21, 2016.

Published OnlineFirst December 21, 2016; DOI: 10.1158/1078-0432.CCR-16-1971

References

1. Huang SX, Jaurand MC, Kamp DW, Whysner J, Hei TK. Role of mutagenicity in asbestos fiber-induced carcinogenicity and other diseases. J Toxicol Environ Health B Crit Rev 2011;14:179–245.
2. Jean D, Daubriac J, Le Pimpec-Barthes F, Galateau-Salle F, Jaurand MC. Molecular changes in mesothelioma with an impact on prognosis and treatment. Arch Pathol Lab Med 2012;136:277–93.
3. Jean D, Jaurand MC. Causes and pathophysiology of malignant pleural mesothelioma. Lung Cancer Management 2015;4:10.
4. Guo G, Chmielecki J, Goparaju C, Heguy A, Dolgalev I, Carbone M, et al. Whole-exome sequencing reveals frequent genetic alterations in BAP1, NF2, CDKN2A, and CUL1 in malignant pleural mesothelioma. Cancer Res 2015;75:264–9.
5. De Rienzo A, Archer MA, Yeap BY, Dao N, Sciaranghella D, Sideris AC, et al. Gender-specific molecular and clinical features underlie malignant pleural mesothelioma. Cancer Res 2015;76:319–28.
6. Bueno R, Stawiski EW, Goldstein LD, Durinck S, De Rienzo A, Modrusan Z, et al. Comprehensive genomic analysis of malignant pleural mesothelioma identifies recurrent mutations, gene fusions and splicing alterations. Nat Genet 2016;48:407–16.
7. Tallet A, Nault JC, Renier A, Hysi I, Galateau-Salle F, Cazes A, et al. Overexpression and promoter mutation of the TERT gene in malignant pleural mesothelioma. Oncogene 2014;33:3748–52.
8. de Reynies A, Jaurand MC, Renier A, Couchy G, Hysi I, Elarouci N, et al. Molecular classification of malignant pleural mesothelioma: identification of a poor prognosis subgroup linked to the epithelial-to-mesenchymal transition. Clin Cancer Res 2014;20:1323–34.
9. Ehmer U, Sage J. Control of proliferation and cancer growth by the Hippo signaling pathway. Mol Cancer Res 2015;14:127–40.
10. Yokoyama T, Osada H, Murakami H, Tatematsu Y, Taniguchi T, Kondo Y, et al. YAP1 is involved in mesothelioma development and negatively regulated by Merlin through phosphorylation. Carcinogenesis 2008;29:2139–46.
11. Mizuno T, Murakami H, Fujii M, Ishiguro F, Tanaka I, Kondo Y, et al. YAP induces malignant mesothelioma cell proliferation by upregulating transcription of cell cycle-promoting genes. Oncogene 2012;31:5117–22.
12. Felley-Bosco E, Stahel R. Hippo/YAP pathway for targeted therapy. Transl Lung Cancer Res 2014;3:75–83.
13. Murakami H, Mizuno T, Taniguchi T, Fujii M, Ishiguro F, Fukui T, et al. LATS2 is a tumor suppressor gene of malignant mesothelioma. Cancer Res 2011;71:873–83.
14. Bott M, Brevet M, Taylor BS, Shimizu S, Ito T, Wang L, et al. The nuclear deubiquitinase BAP1 is commonly inactivated by somatic mutations and 3p21.1 losses in malignant pleural mesothelioma. Nat Genet 2011;43:668–72.
15. Jean D, Thomas E, Manie E, Renier A, de Reynies A, Lecomte C, et al. Syntenic relationships between genomic profiles of fiber-induced murine and human malignant mesothelioma. Am J Pathol 2011;178:881–94.
16. Andujar P, Pairon JC, Renier A, Descatha A, Hysi I, Abd-Alsamad I, et al. Differential mutation profiles and similar intronic TP53 polymorphisms in asbestos-related lung cancer and pleural mesothelioma. Mutagenesis 2013;28:323–31.
17. Rondeau S, Vacher S, De Koning L, Briaux A, Schnitzler A, Chemlali W, et al. ATM has a major role in the double-strand break repair pathway dysregulation in sporadic breast carcinomas and is an independent prognostic marker at both mRNA and protein levels. Br J Cancer 2015;112:1059–66.
18. Troncale S, Barbet A, Coulibaly L, Henry E, He B, Barillot E, et al. NormaCurve: a SuperCurve-based method that simultaneously quantifies and normalizes reverse phase protein array data. PLoS One 2012;7:e38686.
19. Ritchie ME, Phipson B, Wu D, Hu Y, Law CW, Shi W, et al. limma powers differential expression analyses for RNA-sequencing and microarray studies. Nucleic Acids Res 2015;43:e47.
20. Jaurand MC, Jean D. Biomolecular pathways and malignant pleural mesothelioma. In: Mineo CT, editor. Malignant pleural mesothelioma: present status and future directions: Sharjah: Bentham Science Publishers Ltd.; 2016. p. 169–92.
21. Miyanaga A, Masuda M, Tsuta K, Kawasaki K, Nakamura Y, Sakuma T, et al. Hippo pathway gene mutations in malignant mesothelioma: revealed by RNA and targeted exon sequencing. J Thorac Oncol 2015;10:844–51.
22. Cui Q. A network of cancer genes with co-occurring and anti-co-occurring mutations. PLoS One 2010;5:pii: e13180.
23. Thurneysen C, Opitz I, Kurtz S, Weder W, Stahel RA, Felley-Bosco E. Functional inactivation of NF2/merlin in human mesothelioma. Lung Cancer 2009;64:140–7.
24. Fleury-Feith J, Lecomte C, Renier A, Matrat M, Kheuang L, Abramowski V, et al. Hemizygosity of Nf2 is associated with increased susceptibility to asbestos-induced peritoneal tumours. Oncogene 2003;22:3799–805.
25. Jongsma J, van Montfort E, Vooijs M, Zevenhoven J, Krimpenfort P, van der Valk M, et al. A conditional mouse model for malignant mesothelioma. Cancer Cell 2008;13:261–71.
26. Poulikakos PI, Xiao GH, Gallagher R, Jablonski S, Jhanwar SC, Testa JR. Re-expression of the tumor suppressor NF2/merlin inhibits invasiveness in mesothelioma cells and negatively regulates FAK. Oncogene 2006;25:5960–8.
27. Xiao GH, Gallagher R, Shetler J, Skele K, Altomare DA, Pestell RG, et al. The NF2 tumor suppressor gene product, merlin, inhibits cell proliferation and cell cycle progression by repressing cyclin D1 expression. Mol Cell Biol 2005;25:2384–94.
28. Cha HJ, Kim J, Hong SM, Hong SJ, Park JH, Kim ES, et al. Overexpression of renal tumor antigen is associated with tumor invasion and poor prognosis of hepatocellular carcinoma. Ann Surg Oncol 2012;19 Suppl 3:S404–11.
29. Neumann E, Engelsberg A, Decker J, Storkel S, Jaeger E, Huber C, et al. Heterogeneous expression of the tumor-associated antigens RAGE-1, PRAME, and glycoprotein 75 in human renal cell carcinoma: candidates for T-cell-based immunotherapies? Cancer Res 1998;58:4090–5.
30. Sigalotti L, Coral S, Altomonte M, Natali L, Gaudino G, Cacciotti P, et al. Cancer testis antigens expression in mesothelioma: role of DNA methylation and bioimmunotherapeutic implications. Br J Cancer 2002;86:979–82.
31. Zhao B, Ye X, Yu J, Li L, Li W, Li S, et al. TEAD mediates YAP-dependent gene induction and growth control. Genes Dev 2008;22:1962–71.
32. Stein C, Bardet AF, Roma G, Bergling S, Clay I, Ruchti A, et al. YAP1 exerts its transcriptional control via TEAD-mediated activation of enhancers. PLoS Genet 2015;11:e1005465.
33. Liu-Chittenden Y, Huang B, Shim JS, Chen Q, Lee SJ, Anders RA, et al. Genetic and pharmacological disruption of the TEAD-YAP complex suppresses the oncogenic activity of YAP. Genes Dev 2012;26:1300–5.
34. Tanaka I, Osada H, Fujii M, Fukatsu A, Hida T, Horio Y, et al. LIM-domain protein AJUBA suppresses malignant mesothelioma cell proliferation via Hippo signaling cascade. Oncogene 2015;34:73–83.
35. Lopez-Lago MA, Okada T, Murillo MM, Socci N, Giancotti FG. Loss of the tumor suppressor gene NF2, encoding merlin, constitutively activates integrin-dependent mTORC1 signaling. Mol Cell Biol 2009;29:4235–49.
36. Mao JH, Kim IJ, Wu D, Climent J, Kang HC, DelRosario R, et al. FBXW7 targets mTOR for degradation and cooperates with PTEN in tumor suppression. Science 2008;321:1499–502.
37. Hu Y, Carraro-Lacroix LR, Wang A, Owen C, Bajenova E, Corey PN, et al. Lysosomal pH plays a key role in regulation of mTOR activity in osteoclasts. J Cell Biochem 2016;117:413–25.
38. Ou SH, Moon J, Garland LL, Mack PC, Testa JR, Tsao AS, et al. SWOG S0722: phase II study of mTOR inhibitor everolimus (RAD001) in advanced malignant pleural mesothelioma (MPM). J Thorac Oncol 2015;10:387–91.
39. Carracedo A, Ma L, Teruya-Feldstein J, Rojo F, Salmena L, Alimonti A, et al. Inhibition of mTORC1 leads to MAPK pathway activation through a PI3K-dependent feedback loop in human cancer. J Clin Invest 2008;118:3065–74.
40. Barbone D, Yang TM, Morgan JR, Gaudino G, Broaddus VC. Mammalian target of rapamycin contributes to the acquired apoptotic resistance of human mesothelioma multicellular spheroids. J Biol Chem 2008;283:13021–30.

Published OnlineFirst December 21, 2016; DOI: 10.1158/1078-0432.CCR-16-1971

41. Zhou S, Liu L, Li H, Eilers G, Kuang Y, Shi S, et al. Multipoint targeting of the PI3K/mTOR pathway in mesothelioma. Br J Cancer 2014;110: 2479–88.
42. Echeverry N, Ziltener G, Barbone D, Weder W, Stahel RA, Broaddus VC, et al. Inhibition of autophagy sensitizes malignant pleural mesothelioma cells to dual PI3K/mTOR inhibitors. Cell Death Dis 2015;6: e1757.
43. Cheng H, Bagrodia S, Bailey S, Edwards M, Hoffman J, Hu Q, et al. Discovery of the highly potent PI3K/mTOR dual inhibitor PF-04691502 through structure based drug design. Med Chem Commun 2010;1:139–44.
44. Wang FZ, Peng J, Yang NN, Chuang Y, Zhao YL, Liu QQ, et al. PF-04691502 triggers cell cycle arrest, apoptosis and inhibits the angiogenesis in hepatocellular carcinoma cells. Toxicol Lett 2013;220:150–6.
45. Britten CD, Adjei AA, Millham R, Houk BE, Borzillo G, Pierce K, et al. Phase I study of PF-04691502, a small-molecule, oral, dual inhibitor of PI3K and mTOR, in patients with advanced cancer. Invest New Drugs 2014;32:510–7.
46. Del Campo JM, Birrer M, Davis C, Fujiwara K, Gollerkeri A, Gore M, et al. A randomized phase II non-comparative study of PF-04691502 and gedatolisib (PF-05212384) in patients with recurrent endometrial cancer. Gynecol Oncol 2016;142:62–9.

AACR American Association for Cancer Research

Clinical Cancer Research

Co-occurring Mutations of Tumor Suppressor Genes, *LATS2* and *NF2*, in Malignant Pleural Mesothelioma

Robin Tranchant, Lisa Quetel, Anne Tallet, et al.

Clin Cancer Res 2017;23:3191-3202. Published OnlineFirst December 21, 2016.